Bifurcation diagram globally underpinning neuronal firing behaviors modified by SK conductance*

Chen Meng-Jiao(陈梦娇)[a], Ling Heng-Li(令恒莉)[a], Liu Yi-Hui(刘一辉)[a], Qu Shi-Xian(屈世显)[b]†, and Ren Wei(任 维)[a]‡

[a] *Key Laboratory of MOE for Modern Teaching Technology and College of Life Sciences, Shaanxi Normal University, Xi'an* 710062, *China*

[b] *Institute of Theoretical & Computational Physics, School of Physics and Information Technology, Shaanxi Normal University, Xi'an* 710062, *China*

(Received 7 May 2013; revised manuscript received 3 July 2013; published online 10 December 2013)

Neurons in the brain utilize various firing trains to encode the input signals they have received. Firing behavior of one single neuron is thoroughly explained by using a bifurcation diagram from polarized resting to firing, and then to depolarized resting. This explanation provides an important theoretical principle for understanding neuronal biophysical behaviors. This paper reports the novel experimental and modeling results of the modification of such a bifurcation diagram by adjusting small conductance potassium (SK) channel. In experiments, changes in excitability and depolarization block in nucleus accumbens shell and medium-spiny projection neurons are explored by increasing the intensity of injected current and blocking the SK channels by apamin. A shift of bifurcation points is observed. Then, a Hodgkin–Huxley type model including the main electrophysiological processes of such neurons is developed to reproduce the experimental results. The reduction of SK channel conductance also shifts the bifurcations, which is in consistence with experiment. A global bifurcation paradigm of this shift is obtained by adjusting two parameters, intensity of injected current and SK channel conductance. This work reveals the dynamics underpinning modulation of neuronal firing behaviors by biologically important ionic conductance. The results indicate that small ionic conductance other than that responsible for spike generation can modify bifurcation points and shift the bifurcation diagram and, thus, change neuronal excitability and adaptation.

Keywords: neuron, Hopf bifurcation, SK channel, excitability

PACS: 87.19.L–, 87.16.Vy, 87.19.ll, 05.45.–a **DOI:** 10.1088/1674-1056/23/2/028701

1. Introduction

Even a single neuron is a complex physical system. Neurons receive, transform, and output information in the nervous system. The functional output signal of a neuron, by definition, is the action potential.[1] Usually, an action potential occurs when the input to a neuron drives its membrane potential from polarized resting, resting membrane potential state around −80 mV formed by unequal (polarized) distribution of potassium and sodium ions, to a threshold. When the membrane potential increases across this threshold, neuron fires an all-or-none action potential. The generation of one action potential waveform is also termed a firing or a spike. Under input with bigger strength, neurons increase firing frequency and then transit into a depolarized resting, a resting membrane potential state around –15 mV formed by less polarized distribution of potassium and sodium ions. The transition from polarized resting to firing is one threshold, while the transition from firing to the depolarized resting is the other threshold. Because this transition from firing to depolarized resting is caused by the blockage of sodium channel activation, it is also termed a depolarization block.[2] In the working brain, all neurons function between these two thresholds under continuous driving input from its neighbor neurons. Globally, the three states segregated by these two thresholds are polarized resting, various firing pattern, and depolarized resting.[3–6] A general bifurcation diagram including two bifurcation points obtained by using input current as the control parameter has been employed in modeling to globally reveal the dynamics of neuronal firing. In contrast, experimentation purposely covering both of the two bifurcations is rarely reported.

The transition from polarized resting to firing has been investigated in biophysical experiments. Such a transition is generally used to represent intrinsic membrane excitability. By using stepwise current injection the changes in intrinsic membrane excitability have been thoroughly investigated.[7,8] For example, in nucleus accumbens shell (NAcSh) medium-spiny projection neurons (MSNs) mediating emotional and motivational signals by various firing trains, prolonged current injection has been frequently used to study changes in excitability involved in drug abuse. In a series of studies on drug addiction, intrinsic membrane excitability of MSNs has been found to exhibit very rich changes after different co-

*Project supported by the National Natural Science Foundation of China (Grant No. 30900443) and the Fundamental Research Funds for the Central Universities, China (Grant Nos. GK201302052 and GK261001007).

†Corresponding author. E-mail: sxqu@snnu.edu.cn

‡Corresponding author. E-mail: renwei@snnu.edu.cn

© 2014 Chinese Physical Society and IOP Publishing Ltd

caine administration procedures. Afterhyperpolarization potential (AHP) plays an important role in such changes.[9] AHP describes the hyperpolarization phase of an action potential waveform where the membrane potential falls below the normal resting potential. During withdrawal from repeated morphine exposure, intrinsic membrane excitability of MSNs was enhanced and both apamin-sensitive AHP and apamin-insensitive AHP were found to decrease.[10] This experimental evidence implies that there is a relationship between cocaine/morphine withdrawal and variation in AHP. Ion currents underlying AHP are mediated by small-conductance voltage-insensitive Ca^{2+}-activated K^+ channels (SK channels). Recent experiments also found that intrinsic excitability of MSNs was inhibited by changing SK channel conductance during withdrawal from repeated cocaine or amphetamine exposure.[9,11] These indicate a possibility that by adjusting SK channel expression on MSN membranes abused drugs could change intrinsic excitability via adjusting bifurcation from polarized resting to firing.

The transition from firing to depolarized resting has also been investigated in biophysical experiments. For example, in response to prolonged depolarizing current steps, some MSNs showed transition from firing to depolarized resting.[10] The transition from continuous firing to resting induced by increasing injection current is a depolarization block with a dynamics of bifurcation from superthreshold limit cycle oscillation to a resting point,[2] which is commonly seen in the nervous system and is of significant biological importance. For example, a depolarization block appears to be one important mechanism to suppress network hyperactivity,[12] which may be of relevance to originating or spreading of seizures. In addition, antipsychotic drugs achieve their effects by alleviating psychotic features of schizophrenia[13] via inducing depolarization block in dopamine neurons.[14,15]

From the perspective of physics, the dynamics of the above separately obtained experimental results should be explained in consistency. Dynamic modeling has revealed that resting and repeated firing are generated from stable equilibrium and limit cycle attractor, respectively. When the strength of injected current is used as a control parameter, the behavior of their membrane potential oscillation could be driven to evolve between resting and firing. Studies using Hodgkin–Huxley model have reveled that the resting-to-spiking behavior corresponds to a transition away from equilibrium point to a limit cycle. On the other hand, the spiking-to-resting transition corresponds to a transition away from a limit cycle to another equilibrium point. Bifurcation diagram including these two transition provides a general and global paradigm for evolution of firing behavior of neurons.[16] This general paradigm needs to be extended to specific neurons with richer ionic components. The present study will apply this general paradigm to MSNs and provide experimental evidence for further studying the role of SK channels in modifying the bifurcation diagram and the evolution of firing behavior.

In this paper, we report on novel experimental results as well as modeling the results of the modification of a bifurcation diagram underpinning neuronal firing behavior by biologically important ionic conductance. In Section 2 the materials and methods employed in the work are shown. The results are presented in Section 3. The conclusions and discussions drawn from this work are given in Section 4.

2. Materials and methods

2.1. NAcSh slice preparation, cell selection, and electrophysiology

All procedures were performed in accordance with the institutional guidelines for the Care and Use of Laboratory Animals as approved by Animal Care Committee of Shaanxi Normal University. Spragur–Dawley rats (21–30 day old) were anesthetized with chloralhydrate (400 mg/kg, intraperitoneally) and decapitated. Sagittal slices (300 mm) of the nucleus accumbens shell were obtained with a vibratome (Vibratome 1000 plus, Vibratome Company, St. Louis, Missouri, USA) in oxygenated (95% O_2 + 5% CO_2) and ice-cold artificial cerebrospinal fluid (ACSF) containing: 125 mM of NaCl, 3 mM of KCl, 2.4 mM of $CaCl_2$, 1.2 mM of $MgCl_2$, 26 mM of $NaHCO_3$, 1.25 mM of NaH_2PO_4, and 10 mM of glucose. The slices were transferred to a holding chamber and incubated in oxygenated ACSF at room temperature for at least 1 h before recording.

The brain slices were anchored in the recording chamber and perfused with oxygenated ACSF continuously at room temperature (flow rate 1 ml/min–2 ml/min). The cells were visualized using infrared-differential interference contrast optics. MSNs in NAcSh were identified by their morphology and high resting membrane potential (–75 mV to – 85 mV). Standard whole-cell recordings were taken using a MultiClamp 700 B amplifier through an electrode (3 MΩ–5 MΩ) containing 120 mM of K-gluconate, 20 mM of KCl, 10 mM of 4-(2- hydroxyethyl)-1-piperazineethanesulfonic acid, 0.2 mM of ethylene glycol tetra-acetic acid, 4 mM of Na_2ATP, 2 mM of $MgCl_2$, and 0.3 mM of GTP–Tris, at pH 7.2–7.4 (285 mOsm–295 mOsm) in all electrophysiological experiments. Current-clamp recordings were used to measure evoked action potentials, in which the resting membrane potential was normalized to – 80 mV in acute slices. Neurons with their input resistance oscillating at less than 20% were considered to be 'stable' and included for data analysis. The current step protocol was from −200 pA to 400 pA, in steps of 25 pA and 1-s duration; with an inter-pulse interval of 10 s.

2.2. Data acquisition, analysis, and statistics

In response to constant somatic current steps of increasing strength, $I_{\rm inj}$, MSNs fire continuously. In the input range, that values of $I_{\rm inj}$ beyond the range of the linear increase for the I/O curve, MSNs eventually stop firing, reaching a depolarization block in which the membrane potential, during the current injection, keeps constant, generally around −15 mV. It is impossible to obtain the exact current intensity at which neuron just goes through spiking-to-resting behavior in biological experiment, let alone with discontinuous current step stimulation. So, in response to current steps of increasing strength, the amplitude of current injected at which MSN firing at first time reaches the depolarization block within the duration of the current step is considered as the spike-to-resting transition current intensity, $I_{\rm th}$.

In electrophysiological recordings, two to five cells were obtained from one rat. In all experiments, data acquisition, and analysis were performed blindly. Numerical data in the text and error bars in figures were expressed as a mean ± standard error of the mean. Statistical significance was assessed using Student's paired t-test or two-way analysis of variance (ANOVA). A P value of less than 0.05 was considered to be statistically significant.

2.3. Computational model of NAcSh MSN

Simulation is performed using Microsoft Visual C++ and Matlab. The differential equations are solved using the fourth order Runge–Kutta method in steps of 0.01 ms. MatCont software (which is freely available for download at http://www.matcont.ugent.be/) based on Matlab is used for bifurcation analysis. The continuing equilibria, limit cycles (periodic orbits), and their bifurcations (including branch points) of systems of ordinary differential equations (ODEs) are computed with the same prediction–correction continuation algorithm based on the Moore–Penrose matrix pseudo-inverse by MatCont. The continuation of bifurcation points of equilibria and limit cycles is based on bordering method and minimally extended system. MatCont also provides access to all standard ODE solvers supplied by Matlab, as well as to two new stiff solvers, ode78 and ode87. We choose from ode 45, ode78, and ode87 to achieve best precision of computation for bifurcation diagram.

A simple one-compartmental Hodgkin–Huxley-type neuronal model of MSN is constructed. Modified HH model added SK current ($I_{\rm SK}$), SK channels, activated by submicromolar intracellular Ca^{2+}, are selectively coupled with N-type voltage-gated calcium channels, but not other calcium channels,[17,18] then an N-type calcium current ($I_{\rm CaN}$) is added to our models. So, the model contains the sodium current ($I_{\rm Na}$), persistent potassium current ($I_{\rm K}$), leak current ($I_{\rm L}$), N-type calcium current ($I_{\rm CaN}$), and SK current ($I_{\rm SK}$), and is described by the following equation

$$C\frac{{\rm d}V}{{\rm d}t} = I - I_{\rm Na} - I_{\rm K} - I_{\rm L} - I_{\rm CaN} - I_{\rm SK},$$

where

$$\begin{aligned}
&I_{\rm Na} = g_{\rm Na} m^3 h (V - V_{\rm Na}),\\
&I_{\rm K} = g_{\rm K} n^4 (V - V_{\rm K}),\\
&I_{\rm L} = g_{\rm L} (V - V_{\rm L}),\\
&I_{\rm CaN} = g_{\rm CaN} Ca_{\rm N} (k_{mn}/(k_{mn} + [Ca^{2+}]_i))(V - V_{\rm Ca}),\\
&I_{\rm SK} = g_{\rm SK} [Ca^{2+}]_{\rm i}/([Ca^{2+}]_{\rm i} + k_d)(V - E_{\rm K}).
\end{aligned}$$

Here $g_{\rm Na}$, $g_{\rm K}$, $g_{\rm L}$, $g_{\rm CaN}$, and $g_{\rm SK}$ denote the maximal conductance of sodium current, potassium current, leak current, N-type calcium current, and SK current, respectively; V is the membrane potential in millivolts; C is the total membrane capacitance; I is the injected current; $V_{\rm Na}$, $V_{\rm K}$, $V_{\rm L}$, and $V_{\rm Ca}$ are the reversal potentials of their corresponding currents, respectively; m and h are the activation variable and inactivation variable for sodium current, respectively; n is the activation variable for potassium current; and, Ca_N is the activation variable for N-type calcium current.

The gating variables are described as follows:

$$\begin{aligned}
&\frac{{\rm d}m}{{\rm d}t} = \alpha_m(V) - (\alpha_m(V) + \beta_m(V))m,\\
&\frac{{\rm d}h}{{\rm d}t} = \alpha_h(V) - (\alpha_h(V) + \beta_h(V))h,\\
&\frac{{\rm d}n}{{\rm d}t} = \alpha_n(V) - (\alpha_n(V) + \beta_n(V))n,\\
&\frac{{\rm d}Ca_N}{{\rm d}t} = (Ca_{N_\infty}(V) - Ca_N)/\tau_{Ca_N}(V).
\end{aligned}$$

The dynamics of intracellular calcium concentration $[Ca^{2+}]_{\rm i}$ are given by

$$\frac{{\rm d}[Ca^{2+}]_{\rm i}}{{\rm d}t} = -k_1 I_{Ca_N} - k_2 [Ca^{2+}]_i.$$

The parameters for gating variables and calcium dynamics are

$$\begin{aligned}
&\alpha_m(V) = 0.0125(V+30)/(1-\exp(-(V+30)/10.0)),\\
&\beta_m(V) = 0.5\exp(-(V+55.0)/18.0),\\
&\alpha_h(V) = 0.00875\exp(-(V+55.0)/20.0),\\
&\beta_h(V) = 0.125/(1.0+\exp(-(V+25.0)/10.0)),\\
&\alpha_n(V) = 0.00125(V+45.0)/(1-\exp(-(V+45.0)/10.0)),\\
&\beta_n(V) = 0.015625\exp(-(V+55.0)/80.0),\\
&Ca_{N_\infty}(V) = 1.0/(1.0+\exp(-(V+45.0)/7.0)),\\
&\tau_{Ca_N}(V) = 18.0\exp(-(V+70.0)^2/5.0)+0.3.
\end{aligned}$$

The values of the parameters used for simulation are given in Table 1. We use the parameters in the original Hodgkin–Huxley model for the sodium, potassium, and leak currents. These parameters are slightly modified to fit the experimental data of MSNs. However, the mechanisms highlighted are robust to parameter variations, and still hold using the original values. The parameters for the N-type calcium current are cited from Ref. [19].

The global bifurcation can be obtained by adjusting control parameter I. Then, the changing of parameter g_{SK} in modeling and in experiment enables one to explore the role of SK channels in modifying the global bifurcation diagram obtained by adjusting control parameter I.

Table 1. Parameters used in the model.

Parameter	Value	Parameter	Value	Parameter	Value
C	1 pF/cm^2	g_{Na}	200.0 mS/cm^2	k_{mn}	0.0001
V_{Na}	50 mV	g_K	11.0 mS/cm^2	k_1	0.002
V_K	−82 mV	g_L	2 mS/cm^2	k_2	0.00125
V_L	−73 mV	g_{CaN}	2 mS/cm^2	k_d	0.4
V_{Ca}	120 mV	g_{SK}	0.4 mS/cm^2		

3. Results

3.1. Biophysical experimentation

In previous neurophysiological studies of NAcSh MSNs, two types of MSNs have been identified according to their responsiveness to stepwise current injection.[10] In these two types, type II MSNs could be driven by the injected current to transit across the threshold from polarized resting to firing. We experimentally identify type II MSNs to study the bifurcation from an equilibrium point to a limit cycle.

One typical example for responsiveness of NAcSh type II MSN to current injection before and after application of SK channel blocker apamin is shown in Fig. 1(a). Before application of apamin, when the intensity of injected current is 175 pA and less, this type II MSN is still at rest. Then, it fires at following current steps up to 400 pA, and fires throughout the duration of the current step. The current intensity of 200 pA is the resting-to-firing transition current amplitude, named rheobase current amplitude in neurobiology. The rheobase current amplitude decreases to 175 pA after application of apamin.

Since this type II MSN fires continuously when being driven by current injection with intensities up to 200 pA and more, maximum and minimal voltage values of the action potentials can be used to show the relationship between firing amplitude and injected current intensity. An example for this relation of this type II MSN neuron before application of apamin is shown in Fig. 1(b).

In experiment, the MSNs observed show reasonable individual variations. The main conclusion is reached by statistics between different groups. When compared with the control group, a bath application of apamin (100 nM) for 20 min selectively blocking SK channel significantly increases the action potential number [$F(1,22) = 5.882$, $P < 0.05$, $n = 13$, two-way ANOVA; LSD post-hoc test] (Fig. 1(c)) and reduces the rheobase current amplitude (control: 190.3 ± 11.8 pA; apamin: 167.3 ± 9.1 pA, $p < 0.05$ paired t-test) (Fig. 1(d)).

In the observed type I and type II MSNs, type I MSNs could be easily driven by the injected current to transit across the threshold from firing to depolarized resting. We then experimentally identified type I MSNs to study the bifurcation from the limit cycle to another equilibrium point.

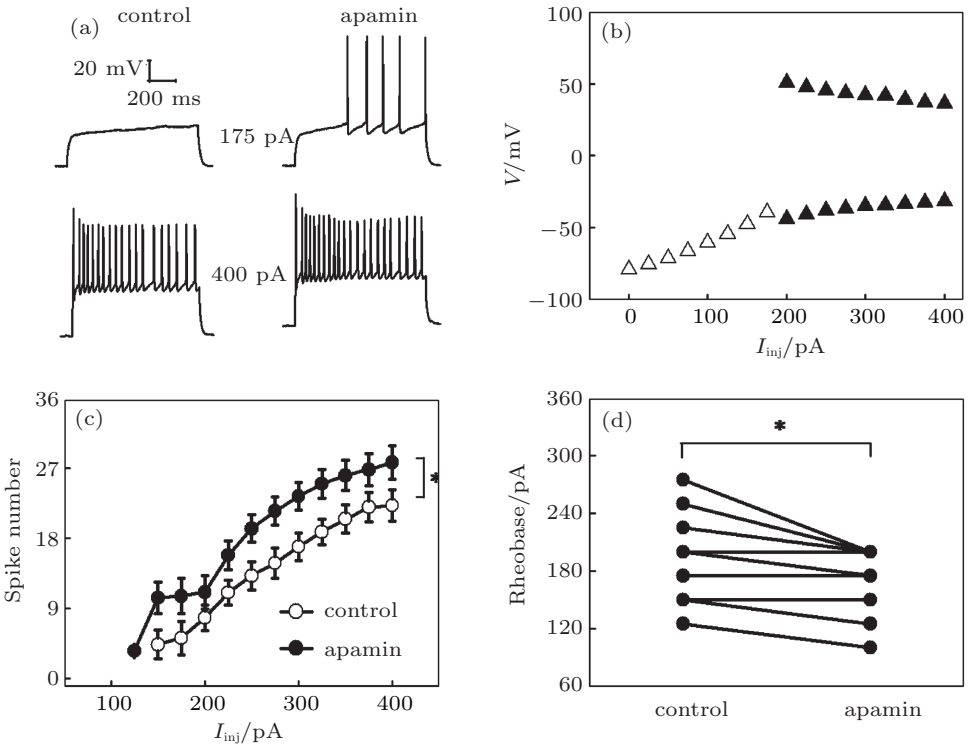


Fig. 1. NAcSh type II MSN spiking patterns in response to increasing current steps. (a) Evoked action potentials induced by 175 pA and 400 pA of injecting currents before and after apamin application in type II MSN. (b) An example for the relation between firing amplitude and injected current intensity of type II before apamin application, Δ: resting potential voltage; ▲: maximum and minimal voltage values of the action potentials. (c) Bath application of apamin significantly increases the number of evoked spikes. (d) Bath application of apamin significantly reduces the rheobase current amplitude. $n = 13$ and $^*P < 0.05$.

A typical example for responsiveness of NAcSh type I MSN to current injection before and after application of SK channel blocker apamin is shown in Fig. 2(a). Before application of apamin, when the intensity of injected current is increased to 75 pA and more, this type I MSN exhibits continuous firing. When the intensity of the injected current is increased to 225 pA, it cannot fire continuously throughout the duration of current step. Near this current intensity this type I MSN is driven to transit across a bifurcation from the limit cycle to a depolarized equilibrium point. In experimentation, the current intensity of 225 pA is defined as the firing-to-resting transition current amplitude, $I_{\rm th}$. The value of $I_{\rm th}$ decreases to 175 pA after application of apamin.

The relationship between firing amplitude and injected current intensity of this example type I MSN is shown in Fig. 2(b). When injected current intensity is less than 75 pA, this example type I MSN stays at a polarized resting equilibrium point. When the injected current intensity is between 75 pA and 225 pA, this neuron fires throughout the duration of current injection. When injected current intensity is larger than 225 pA, this neuron stays at a depolarized resting equilibrium point.

By comparison with control, bath application of apamin (100 nM) for 20 min selectively blocking SK channels significantly reduces the threshold intensity of transition from firing to depolarized resting, $I_{\rm th}$ (control: 278.5 $\pm$ 25.8 pA; apamin: 232.1 $\pm$ 24.2 pA, $p < 0.01$ paired t-test, $n = 8$) (Fig. 2(c)).

The above experimental results show that the input–output functions of both type I and type II MSNs are modulated by SK channels. This action is achieved by changing the membrane potential to make it more depolarizing by mediating a potassium ion efflux.

In both the present and a series of previous experiments, type I MSNs can be stimulated to transit across two thresholds and exhibit adaption, while type II MSNs are able to transit across only the transition from resting-to-spiking and exhibit no adaptation.[10] Such a difference results from the difference in expression between ion channels and neurotransmitter receptors, including dopamine receptor,[20] in these two types of MSNs. Such a different expression may explain the difference in the effect of SK channel blocker on firing dynamics between the two types of MSNs.

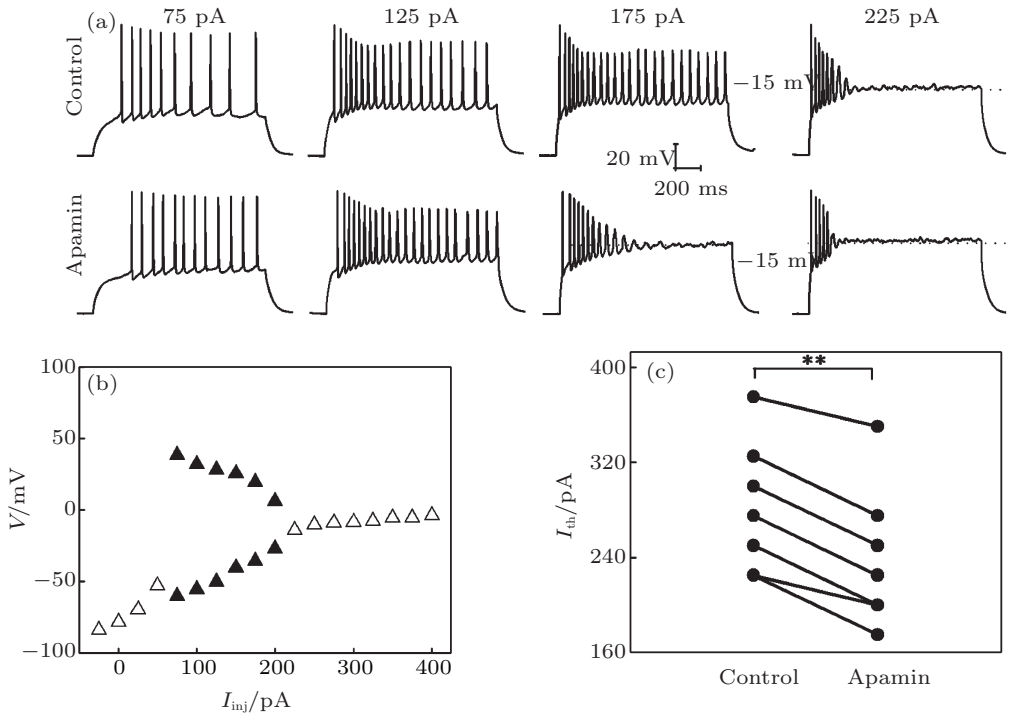


Fig. 2. NAcSh type I MSN spiking patterns in response to increasing current steps. (a) Evoked action potentials induced by 75, 125, 175, and 225 pA of injecting currents before and after apamin application in type I MSN. (b) An example for the relation between firing amplitude and injected current intensity of type I MSN before apamin application, Δ: resting potential voltage; ▲: maximum and minimal voltage values of the action potentials. (c) Bath application of apamin significantly reduces $I_{\rm th}$. $n = 8$ and $^{**}P < 0.01$.

3.2. Dynamic modeling

The MSN model that was previously described in our material and methods section is employed to reproduce the above experimentally observed results. To be in consistence with the above experimentation, where apamin is used to modify the bifurcations driven by adjusting parameter $I_{\rm inj}$, and $g_{\rm SK}$ and I are used as modification and bifurcation parameter, respectively. The units of $g_{\rm SK}$ and I are mS/cm^2 and pA, respectively. $g_{\rm SK}$ is kept at 2.8 to simulate the experimental observation before application of apamin, and then changed into 0.4 to simulate

the experimental results after apamin application.

Two experimental processes, one before and the other after apamin application, are simulated and shown in Fig. 3(a). The range of injected current intensity is from 75 pA to 225 pA. Changing g_{SK} from 2.8 to 0.4, I_{th}, which is the threshold corresponding to bifurcation from limit cycle to depolarized equilibrium, is modified from 225 pA to 175 pA. The dynamic model used in the present study is one-compartmental, which enables us to perform dynamic analysis on bifurcation but introduces slight difference in the above parameter range as compared with experiment. Simplification of the three-dimensional morphological structure affects the RC time constant and the specific point of bifurcation.[21]

The 'global' bifurcation diagram driven by adjusting I with g_{SK} set at 2.8 is shown in Fig. 3(b). There are two Hopf bifurcations (HB) points. The first HB point corresponds to a subcritical Hopf bifurcation; that is, a phenomenon which occurs when a stable equilibrium point becomes unstable with the emergence of a stable limit cycle. Beyond it, the neuron exhibits a regular train of firing. When I increases, the amplitude of the firing oscillations decreases and finally reaches the second HB point, which is a supercritical Hopf bifurcation. The membrane potential reaches an equilibrium point; that is, depolarization block.

In experiment, I_{th} obtained from a number of tested neurons ($n = 8$) shows an obvious individual difference. However, apamin application changes I_{th} for all of the neurons tested. We then set the values of g_{SK} to be 20, 11, 8, 6, 4, and 2.8. Then we reduce the values of g_{SK} into 15, 6, 4, 2.8, 1.2, and 0.4, respectively, to simulate I_{th} changes seen in each individual neuron before and after bath application of apamin. The simulation result is shown in Fig. 3(c), which is consistent with the experimental result.

Finally, we simulate 'globally' the firing behavior by adjusting two parameters g_{SK} and I. As shown in Fig. 4, in the region below 25 mS/cm^2 (which is reasonable in neurobiology), between the two bifurcation points MSNs generate continuous firing, and parameter I_{HB1} and I_{HB2} shift toward smaller values when parameter g_{SK} is reduced. This diagram clearly indicates the dynamics underpinning the experimental results.

Within the range of current injected in experiment, type I MSN has two thresholds and three states that are polarized resting, firing, and depolarized resting, respectively. Type II MSN has only one threshold and two states that are polarized resting and firing. However, 2-paramter bifurcation diagram suggests that Type II MSN should have the second threshold, but this is out of the experimental window. To test this prediction experimentally, we perform electrophysiological recordings on rat brain slices. The amplitudes of current injected is even stepped to 1000 pA.[12] Different type II MSNs enter into depolarized blocks at different current steps (unpublished data).

Dependence of the dynamical properties of the model varying with I and g_{SK} in the intervals [0, 450] pA and [0, 25] mS/cm^2, respectively. I_{HB1} and I_{HB2} decrease with the reduction of g_{SK}.

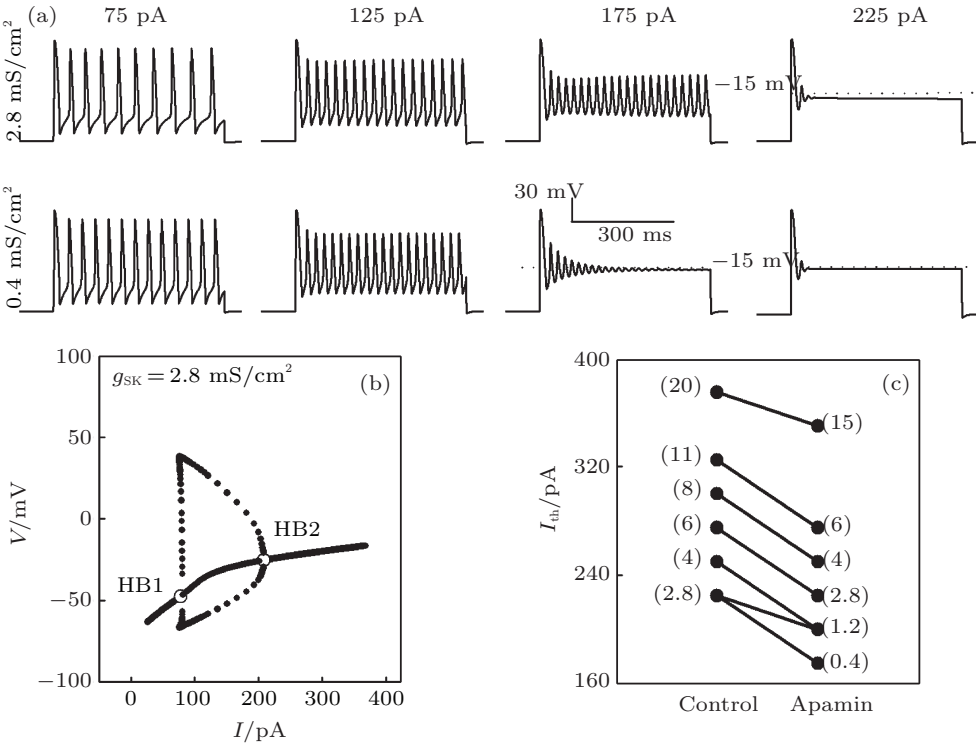


Fig. 3. (color online) Simulations of MSN spiking patterns in response to increasing current steps. (a) Simulated action potentials evoked by 75, 125, 175, and 225 pA of injecting currents when the values of g_{SK} are 2.8 and 0.4, respectively. (b) The 'global' bifurcation diagram driven by adjusting I with g_{SK} set to be 2.8. ◯: HB point; •: maximum and minimal voltage values of the action potentials; solid line: stable equilibrium point; grey line: unstable equilibrium point. (c) Simulation of I_{th} reduction by reducing g_{SK} of each MSN, data in bracket are the values of g_{SK}.

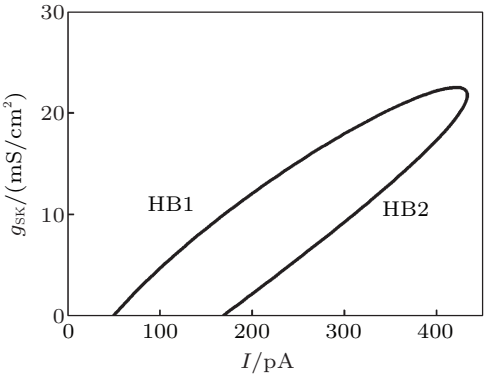


Fig. 4. The 2-parameter bifurcation diagram.

4. Conclusion and discussion

In this paper, we report on novel experimental and numerical result of modification of the bifurcation diagram underpinning neuronal firing behavior. Previous investigations have proposed that a general bifurcation diagram can be employed to explain the changes in neuronal firing patterns.[3,5,22–24] Such findings lead to important improvements in theoretical understanding of physical principles governing neuronal biophysical behaviors. Our present work further focuses on the modification of the general bifurcation diagram to reveal dynamics underpinning modulation of neuronal firing behaviors by biologically important ionic conductance. The results indicate that some small ionic conductance other than those responsible for spike generation, such as the SK conductance studied in this paper, can modify bifurcation points and shift the bifurcation diagram and thus change the excitability and adaptation of neurons. This enriches the understanding of bifurcation dynamics underpinning neuronal encoding.

The findings provided in the present study should be of help for deeper understanding of a number of neurobiological phenomena, such as adaptation in MSN firing behaviors and its changes after chronic administration of abused drugs. A promotion of adaptation in MSN is found after cocaine or amphetamine application or chronic morphine withdrawal.[10,25] Our results give not only a possible pathway of the action of abused-drugs, SK channel, but also a dynamic mechanism, modification of bifurcation from limit cycle to depolarized equilibrium, for such experimental observations.

The transition from limit cycle to depolarized equilibrium, that is, depolarization block in biology, has gradually drawn more attention because of its biological function. In a visual system, there are two types of photoreceptors in the human retina: rods, and cones. In a dark environment, rods are responsible for vision and the cones are inactive (scotopic vision). In the light, however, cones are active (photopic vision) and the rods enter into a depolarization block. In a central nervous system the depolarization block also plays an important role in suppressing network hyperactivity, which sometimes destroys the network stability and leads to over-excitability.[12]

Experimental study demonstrates that the intrinsic excitability, usually measured by rheobase and firing frequency, of a neuron is adjustable. In a series of studies on drug addiction, intrinsic membrane excitability of MSN has been found, exhibiting very rich changes after different cocaine administration procedures. More generally, neuronal output is determined by both synaptic input and intrinsic neuronal excitability. It has been widely documented that dynamic changes in both the synaptic strength and the intrinsic excitability of MSN in the NAc contribute to the development and/or relapse of drug addiction.[9,25–27] Some researches indicate that the spike adaptation is also dynamic, which is caused by the transition from limit cycle to the depolarized resting. Our previous study showed that the selective activation of GluN2A or GluN2B-containing NMDARs enhanced the spike adaptation or intrinsic excitability, respectively.[11] Chronic withdrawal from repeated morphine exposure induces a trichotomous modification in the membrane properties of NAcSh MSNs in a cell type-specific manner, an enhancement of intrinsic excitability in type II neuron, and a promotion of spike adaptation in type I neuron.[10] All of these previous results now can be understood more deeply with help of the conclusion of the present study.

A number of simple models with only a few variables,[28–30] like the one constructed by Izhikevich,[28–30] are not only successful in reproducing many neuronal firing behaviors but also convenient in bifurcation analysis. Although the main phenomena of our present experimentation can also be qualitatively simulated by using such simple models (data not shown here), in this study we employ an HH type model, which includes six variables and many ionic conductance parameters to realistically reproduce the experimental processes. Such reproduction targeting specific channels can guide further experiment and link experiment with theories. Deeper theoretical study on dynamics on shifts of bifurcation needs to be done with simpler models in the future.

References

[1] Hille B 2001 *Ion Channels of Excitable Membranes,* 3rd edn. (Sunderland, MA: Sinauer Associates) p. 27
[2] Izhikevich E M 2007 *Dynamical Systems in Neuroscience: The Geometry of Excitability and Bursting*, 2nd edn. (Massachusetts, Cambridge: MIT Press) p. 118
[3] Wu X B, Mo J, Yang M H, Zheng Q H, Gu H G and Ren W 2008 *Chin. Phys. Lett.* **25** 2799
[4] Yooer C F, Wei F, Xu J X and Zhang X H 2011 *Chin. Phys. Lett.* **28** 030501
[5] Li L, Gu H G, Yang M H, Liu Z Q and Ren W 2004 *Int. J. Bifur. Chaos* **14** 1813
[6] Men C, Wang J, Qin Y M, Wei X L, Che Y Q and Deng B 2011 *Chin. Phys. B* **20** 128704

[7] Xu J, Kang N, Jiang L, Nedergaard M and Kang J 2005 *J. Neurosci.* **25** 1750

[8] Jung S C and Hoffman D A 2009 *Plos One* **4** e6549

[9] Mu P, Moyer J T, Ishikawa M, Zhang Y, Panksepp J, Sorg B A, Schlüter O M and Dong Y 2010 *J. Neurosci.* **30** 3689

[10] Wu X B, Shi M M, Ling H L, Wei C L, Liu Y H, Liu Z Q and Ren W 2013 *Brain Res. Bull.* **90** 92

[11] Shi M M, Wu X B, Wei C L, Yang M H, Liu Z Q and Ren W 2011 *Neuroreport* **22** 762

[12] Bianchi D, Marasco A, Limongiello A, Marchetti C, Marie H, Tirozzi B and Migliore M 2012 *J. Comput. Neurosci.* **33** 207

[13] Valenti O, Cifelli P, Gill K M and Grace A A 2011 *J. Neurosci.* **31** 12330

[14] Boye S M and Rompré P P 2000 *J. Neurosci.* **20** 1229

[15] Grace A A, Bunney B S, Moore H and Todd C L 1997 *Trends Neurosci.* **20** 31

[16] Dovzhenok A and Kuznetsov A S 2012 *Plos One* **7** e42811

[17] Kasten M R, Rudy B and Anderson M P 2007 *J. Physiol.* **584** 565

[18] Alvina K and Khodakhah K 2008 *J. Physiol.* **586** 2523

[19] Canavier C C and Landry R S 2006 *J. Neurophysiol.* **96** 2549

[20] Kim J, Park B H, Lee J H, Park S K and Kim J H 2011 *Biol. Psychiat.* **69** 1026

[21] Wolf J A, Moyer J T, Lazarewicz M T, Contreras D, Benoit-Marand M, O'Donnell P and Finkel L H 2005 *J. Neurosci.* **25** 9080

[22] Chay T R, Fan Y S and Lee Y S 1995 *Int. J. Bifur. Chaos* **5** 595

[23] Fan Y S and Chay T R 1994 *Biol. Cybern.* **71** 417

[24] Chay T R 1985 *Physica D* **16** 233

[25] Kourrich S and Thomas M J 2009 *J. Neurosci.* **29** 12275

[26] Brebner K, Wong T P, Liu L, Liu Y, Campsall P, Gray S, Phelps L, Phillips A G and Wang Y T 2005 *Science* **310** 1340

[27] Kourrich S, Rothwell P E, Klug J R and Thomas M J 2007 *J. Neurosci.* **27** 7921

[28] Izhikevich E M 2003 *IEEE Trans. Neural Netw.* **14** 1569

[29] Wang Z L 2008 *Acta Phys. Sin.* **57** 4771 (in Chinese)

[30] Qin Y M, Wang J, Men C, Zhao J, Wei X L and Deng B 2012 *Chin. Phys. B* **21** 078702